

Prediction of Global, Diffused and Direct Solar Radiation for Oriented and Inclined Surface Based on Meteorological Data for efficient energy use in the south of Tunisia

Mahmoud Ben Amara ¹⁻², Elhem Rdhaounia ¹⁻², Moncef Balghouthi ¹

1-Thermal Process Laboratory (LPT), Research and Technology center of Energy (CRTEn), Bordj-Cedria, Tunisia.

2-Physics department, Faculty of sciences, University of Gabes (UnivGb), Tunisia

Abstract-The determination of solar radiation data at a given geographic location is critical for the development and evaluation of solar applications. The current paper compares a "MATLAB" simulation model with climatology measured data for ten years provided by a high precision meteorological station installed in Tataouine (32° 93' latitude, 10° 45' longitude) in Tunisia's south, where available solar resources are very important. On hourly, monthly, and seasonal scales, the global and direct solar radiation variability was assessed. In order to determine the model's performance, a statistical test method was used. It shows a good potential for estimating values of solar radiation components on various types of surfaces in nearby locations where sunlight measurements aren't available. Such accurate knowledge is very useful for the site selection of solar power plants for both photovoltaic and concentrated thermal systems.

I. INTRODUCTION

Energy consumption is increasing over time, so it is so necessary to find a useful long-term and eco-friendly source: the solar energy is the important alternative; it is plentiful, renewable, widely distributed and clean.

Many applications of solar energy design in various field such as; environmental, remote sensing, climatology, ecology, science, building design, photovoltaic and land management [1] and [1]. Require the average values of global irradiances on different surfaces on an hourly, daily, and monthly basis. In addition, atmospheric physicists and meteorologists need solar radiation data in their research, the major problem always is the non-availability of this data for many areas. Some countries had an expensive radiation measuring equipment installed at different local's stations for meteorological purposes, this continuous running of such network could be costly and a time-consuming operation because of maintenance, regular checking, data collection...

In addition, lack of data and lack of appropriate modeling tools needed to drive such formulations, and all these difficulties have led scientists to use uncomplicated models, for solar radiation estimation.

Many studies are being conducted in various parts of the world to assess the solar potential, and much progress has been made recently in estimating and modeling solar radiation. In fact, we find in the literature, many authors who tried to develop numerous models for solar radiation forecasting.

Zhang et al. [2], proposed and developed many mathematical formula-based models, such as empirical models and artificial intelligence techniques, and conducted

a critical review of existing models for estimating and forecasting solar radiation in the literature. They compared the models in terms of forecasting over time horizons.

Nwokolo and Ogbulezie [3], presented a review paper that provided distinct and reliable results for various approaches as empirical and soft computing model.

Makade et al. [4] proposed a theory-based method for predicting monthly average global solar radiation for the Indian subcontinent, as well as a Prediction of global solar radiation using a single empirical model for a variety of locations across India.

Blal et al. [5], suggested a global solar radiation models suitable for different locations around Adrar city in Algeria.

Kurniawan [6], developed an accurate model to estimate solar radiation, particularly in locations where measured data is unavailable. This model was validated by comparing estimation results to measured solar radiation data at five different stations in Japan.

We can also find software packages that allow us to forecast solar flux density at various locations where no equipment is available.

Testing such as methodology is very interesting, for estimating the irradiation potential necessary for modeling photovoltaic systems in numerous stations distributed in Tunisia where the metrologically data in not a valuable; to robust assess to smart energy that is eco-friendly

This study aims to estimate the global, direct and diffuse hourly solar radiation on an oriented and inclined surface in the south of Tunisia. The prediction was made by modeling based on data from a very high precision weather station installed in the city of Tataouine. In addition, almost of all photovoltaic and thermal solar collectors installed in Tunisia are oriented towards the south with a fixed angle of inclination of 35. Thus, another objective of this work is to make it possible to determine the optimal orientations throughout year-round. This will allow installers in southern Tunisia to choose the optimal orientations or to offer flexible orientations according to the period or the seasons.

II. SITE DESCRIPTION

Tunisia with an area of 163,610 km² is located in North Africa bordered on the west by Algeria, on the south-east by Libya and by the Mediterranean Sea on the north and east "Fig.1".

The southern regions of Tunisia have a Saharan dry climate with a good renewable energy potential, particularly solar radiation, which ranges from 1800 kWh.m⁻² per year in the north to 2800 kWh.m⁻² per year in the south. In terms of global solar radiation, the daily average is between 4.2 kWh.m⁻² per day in the north west to 5.4 kWh.m⁻² per day in the far south, with most of the country (over 80%) located in the upper fringe of 4. [7].

The data for this study was collected at a location called Tataouine, which is located in Tunisia's southern Saharan desert. The geographical distribution of this station is depicted on the map in "Fig.1", and more information can be found in Table 1.



Figure 1. Map of Tataouine, Tunisia

Table 1. Geographically parameters of Tataouine, Tunisia

Latitude(φ)	Longitude (λ)	Altitude (e)	Time zone
32°55'46.81"N	10°27'6.37"E	0.21 km	GMT +1h



Figure 2. High Precision Meteorological Station installed in the site of Tataouine, Tunisia.

III. METEOROLOGICAL SOLAR STATION

The global horizontal solar irradiance, the direct normal irradiation and the diffuse irradiation has been measured during the period from 2010 to 2018 using a high precision meteorological station for solar resource assessment installed in Tataouine "Fig.2".

At a height of 10 meters, the meteorological station measures direct, diffuse, and global irradiance, relative humidity, air temperature, barometric pressure, and wind speed and direction. The solar radiation measuring equipment's of this station are installed on a two-axis support, which can follow the path of the sun. The rotations of the support are controlled by software linked to the global

positioning system "G.P.S". The readjustment of the orientation towards the sun is done using a date file (day, hour, minute) in addition to the sensors based on photovoltaic cells. The data collected by the station are sent daily via an internet network to the Energy Research and Technology Center of BorjCedria, Tunisia.

The measurement of the Global Horizontal Irradiance (w.m⁻²) and the Diffuse Horizontal Irradiance (w.m⁻²) at ground was performed by K&Z CMP21 pyranometer, when the Direct Normal Irradiance (w.m⁻²) is measured from the K&Z CHP1 pyrheliometer "Fig.3a".

The Ambient temperature (°C) and the relative humidity (%) are measured with Campbell CS215 probe "Fig.3b" there is also Anemometer NRG 40H for the measure of the wind speed (m.s⁻¹) and Sensor NRG 200 for the wind direction (°N) (to East) "Fig.3c". For air pressure measurements there is Campbell CS100 sensor "Fig.3d". The Table.2, summarize the accuracy of each used sensors.

The data illustrated in "Fig.3a, 3b, 3c, 3d" present the variation of horizontal global, diffuses direct normal irradiation, temperature, relative humidity, wind parameter and atmospheric pressure for arbitrary day of the year 2018 in clear sky conditions, all of this shows that the meteorological station of Tataouine provide good information with high precision which will be useful for the validation of numerical models.

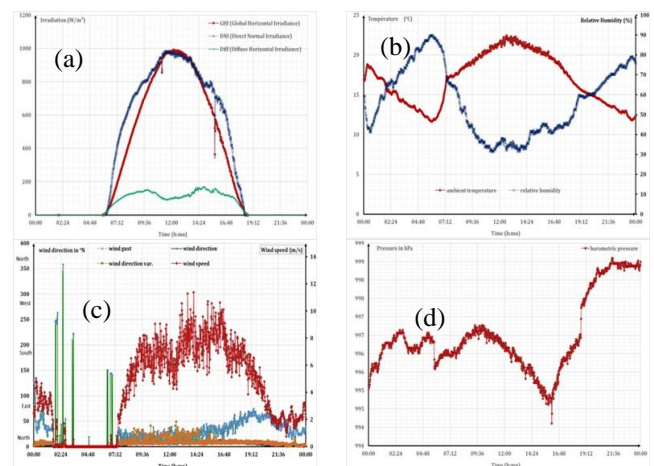


Figure 3: The data collected by the high precision meteorological station of Tataouine for arbitrary day of the year in clear sky conditions (a) Observed horizontal global, diffuses and direct normal irradiation. (b) Observed relative humidity and temperature (c) Observed wind parameter (d) Observed atmospheric pressure.

Table.1. The accuracy of each used sensors

Sensor	Type	accuracy
Pyrheliometer	Kipp&Zonen CHP1	±1 W/m ²
Pyranometer	Kipp&Zonen CMP21	±7 W/m ²
Temperature and Relative Humidity Probe	Campbell Scientific CS215	±0.9°C over -40°C to +70°C ±2% over 10 to 90%
Anemometer	NRG #40C	< 0.1 m/s over 5 to 25 m/s
Wind vane	NRG #200P	< 1%

After data filtering and quality control of the results of the measured frequencies of irradiation, ambient temperature and wind speed overall a year in clear sky conditions, illustrated in "Fig.4, 5 and 6", we can say that the site of

Tataouine then the south of Tunisia in general, present an important solar potential with favorable climatic conditions, in fact:

- Direct solar radiation has exceeded the value of 700 w.m^{-2} for 1700 hrs. by a year, same for the global solar radiation it has exceeded 700 w.m^{-2} during 1600 hrs. by a year. while diffuse solar radiation present the large number of hours for values lower than 400 w.m^{-2} “Fig.4”
- The ambient temperature varied between 20 and 25°C most of the time and we have up to 6000 hours by year of ambient temperature greater than 20°C “Fig.5”
- Concerning the wind speed, it is observed from “Fig.6” that up to 6897 hours by year, wind speed is inferior to 4 m.s^{-1}

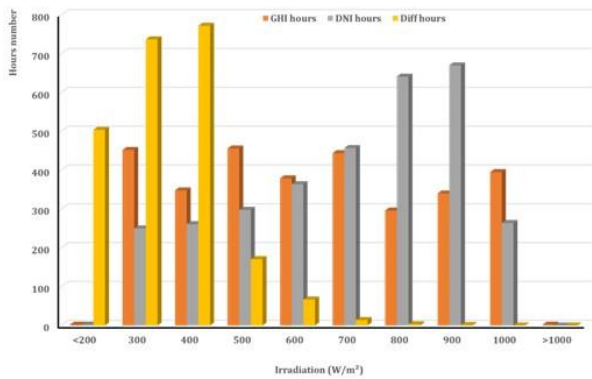


Figure 4: Frequencies of irradiation measured by the high precision meteorological station of Tataouine overall a year in clear sky conditions.

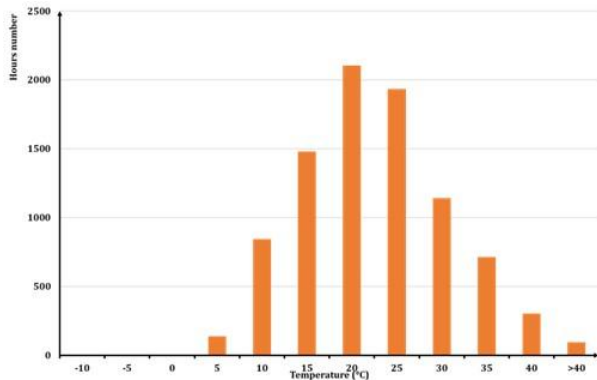


Figure 5: Frequencies of ambient temperature measured by the high precision meteorological station of Tataouine overall a year in clear sky conditions.

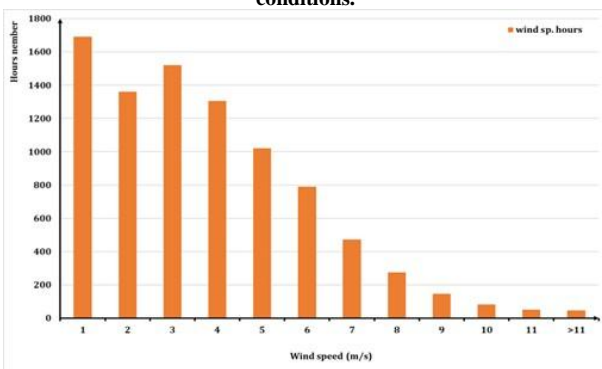


Figure 6: Frequencies of wind speed measured by the high precision meteorological station of Tataouine overall a year in clear sky conditions

IV. CALCULATION OF SOLAR RADIATION FOR INCLINED AND ORIENTED SURFACE

Solar irradiation is the total amount of light and energy emitted by the sun. It is made up of two parts: a direct component (DI) and a diffuse component (Diff), which combine to form the Global Solar Radiation (GI),

The inclination and orientation of the surface determine the total amount of solar irradiation received by the earth; all of these are calculated with (w.m^{-2}).

A. Direct Solar Radiation (In Clear Sky Conditions)

Direct Solar Irradiation (DI) is sunlight that passes directly through the atmosphere to the earth's surface, and it is calculated theoretically using the following formula when it is received by an inclined surface with a south-facing orientation “Fig.7”.

$$DI(\theta, \gamma) = DI(\sin(h) \cos(\theta) + \cos(h) \cos(\gamma - \alpha) \sin(\theta)) \quad \text{Eq.1}$$

Where h (degrees) is the height of the sun, α (degrees) is the azimuth with the south, θ (degrees) is the inclination angle of the receiver with the horizon, γ (degrees) is the orientation of the receiver surface with the south and DI (w.m^{-2}) is the direct irradiation corrected by the atmospheric phenomena received by an horizontal surface.

The azimuth α is the angle between the meridian of the place and the vertical plane passing through the sun; it given by the following equation:

$$\alpha = \arcsin\left(\frac{\cos \Delta}{\cos h}\right) \quad \text{Eq.2}$$

Eq. 3 corrected the direct solar irradiation DI , can be calculated by the Kasten formula [8], [9] .

$$DI = (C - 31K) \exp\left(\frac{-AK}{0.9A + 9.4}\right) \quad \text{Eq.3}$$

The value chosen for C (w.m^{-2}) is 1367 w.m^{-2} , where C (w.m^{-2}) is the normal incidence extraterrestrial [10]. Where A is the relative optical air mass and K is the turbidity atmospheric factor for clear skies.

The Link turbidity factor K is influenced by the Angstrom turbidity coefficient β and by the columnar water vapor content v (cm) of the atmospheric as given by Eq. 4, the empirical formula [10]

$$K = 1.6 + 1.6\beta + 0.5 \ln\left(\frac{v}{0.17}\right) \quad \text{Eq.4}$$

The relative optical air mass A (Eq. 5), is given function the atmospheric pressure P (mbar), the height of the sun h (degrees) and the elevation of such site e (km)[8]

$$A = \frac{P}{1013} \frac{(0.88)^e}{\sin h} \quad \text{Eq.5}$$

The atmospheric pressure at sea level is related to the elevation by Eq.6

$$P = 1013.25 \exp(-0.000118e) \quad \text{Eq.6}$$

The height of the sun h is the angle formed by the horizontal plane at the place of observation and the direction of the sun. It is given by Eq.7[11].

$$h = \arcsin(\sin \phi \sin \Delta + \cos \phi \cos \Delta \cos w) \quad \text{Eq.7}$$

Where ϕ (degrees) is the latitude of the studied site, w (degrees) is the hour angle of the sun, and Δ (degrees) is the angle between the sun's direction and the equatorial plane called the solar declination, it can be calculated by the approximate formula (Eq.8) given by [12]

$$\Delta = \left(\frac{180}{\pi} \right) \arcsin \left(\sin \pi \frac{23.45}{180} \sin \left(278.97 + \frac{360}{365.25} i + 1.9165 \sin \left(356.6 + \frac{360}{365.25} i \right) \right) \right) \quad \text{Eq.8}$$

This formula considers the elasticity of the Earth's trajectory with i is the number of the day of year starting from the first of January.

w (degrees) is given by Eq. 9.

$$w = 15(V - 12) \quad \text{Eq.9}$$

V (hours) is the true solar time of the study site, it is can be calculated by the following:

$$V = L + T \quad \text{Eq.10}$$

L (hours) is the local solar time of the studied site, it is given by Eq.11

$$L = \text{GMT} + \frac{\lambda}{15} \quad \text{Eq.11}$$

Where GMT (hours) is the universal time, λ is the longitude at local studied (degrees), in this case L is $10^\circ 49'$, and T is the equation of time which is known by the difference between local solar time L and true solar time V , we use the expression (Eq.12) proposed by [13].

$$T = 229.2(0.000075 + 0.001868 \cos \tau - 0.032077 \sin \tau - 0.014615 \cos 2\tau - 0.04089 \sin 2\tau) \quad \text{Eq.12}$$

$$\text{Knowing that } \tau = \frac{360}{365}(i - 1) \quad \text{Eq.13}$$

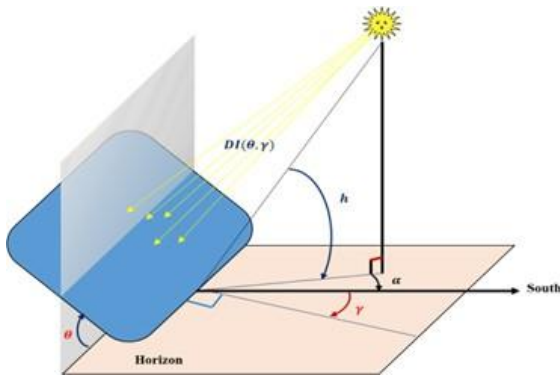


Figure 7. Schematic representation of the inclined and oriented surface.

B. Diffuse solar radiation (in clear sky conditions)

The Diffuse Solar Irradiation Diff (w.m^{-2}), is radiation that has been scattered out of the direct beam, It is given by Eq.14[14]

$$\text{Diff} = 380 \exp\left(\frac{-4}{K}\right) \exp\left(\frac{-e}{7.8}\right) (\sin h)^{(K+6)/30} \quad \text{Eq.14}$$

C. Global Solar Radiation (In Clear Sky Conditions)

To calculate the global solar radiation GI (w.m^{-2}), we use the formula proposed by a commission of the world meteorological organization (Eq.15)[15]

$$GI = (1300 - 57K) \exp\left(\frac{0.22e}{7.8}\right) (\sin h)^{(K+36)/33} \quad \text{Eq.15}$$

V. RESULTS AND DISCUSSION

A. Solar Irradiance on Horizontal Surfaces

After data filtering, we employed the measured data of hourly, daily and monthly average of the horizontal global, diffuse and direct normal irradiances. The measurements are done on horizontal surface and we used data for all the months of the year 2018 of the High Precision Meteorological station of Tataouine. Detailed comparison

against carefully measured data is a good way to assess the performance of a simulation model. An example of such a comparison will be provided here, using the dataset measured by the High Precision Meteorological Station of Tataouine under the auspices of Tunisian Research and Technology Center of Energy.

For the validation, we have used “MATLAB”. Also, we have developed programs allowing a daily prediction of the global, diffuse and direct solar irradiances. From each of these programs, the representative curves of the measured and the estimated values by the numerical model are prepared and presented in the same diagram.

The simulation proposed in this paper was tested for horizontal surface in Tataouine city. We present the recorded and estimated values under clear sky conditions of the hourly horizontal global, horizontal diffuses and direct normal irradiances for a representative day of the selected month. Except in cloudy skies, the proposed model provides a good approximation throughout the year,

According to the “Fig.8a, 8b, 8c, 8d” and Table 2 illustrating the global, diffuse and direct solar irradiances, during a representative month of each season (winter, spring, summer and autumn) in clear sky conditions, except for sunrise and sunset when the sun is low in the sky, the mean relative difference in 2018 has decreased.

This explains why the previously mentioned general expressions for calculating solar irradiation include the factor of atmospheric turbidity [8], [16], which is defined as a function of absorption and extinction coefficients to atmospheric constituents such as ozone O_3 , water vapor (H_2O to gaseous state) [17], aerosols, air molecules, and other gases (O_2 , CO_2) [18].

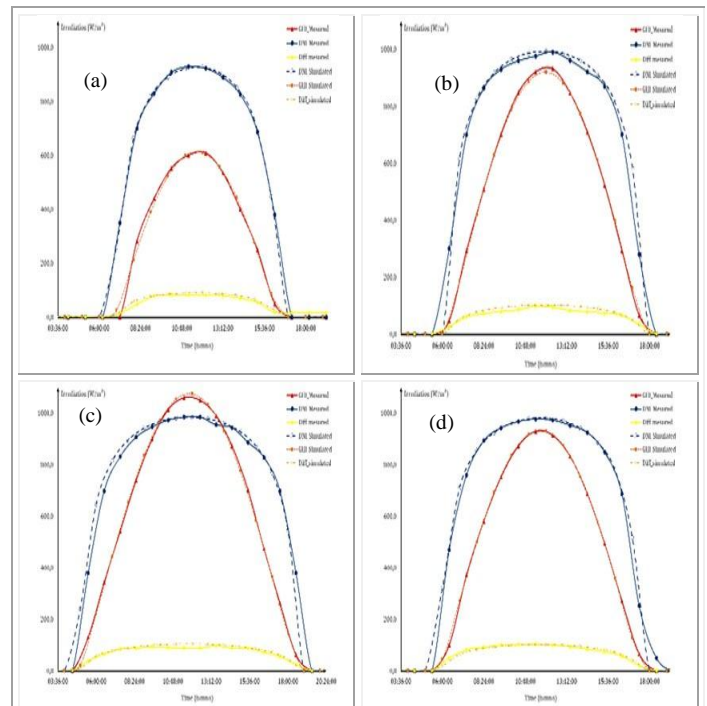


Figure 8. Modeled and measured mean monthly global radiation for the representative month of each season (a) during Winter (8 December 2018) (b) during Spring (17 May 2018) (c) during Summer (21 June 2018) (d) during Autumn (21 September 2018).

Table 2. Modeled and measured mean monthly global radiation for the representative month of each season.

Season	Winter 2018 Dec.8	Spring 2018 Ma.17	Summer 2018 Jun.21	Autumn 2018 Sep.21
Curves	(a)	(b)	(c)	(d)
Measured values(w.m^{-2})	GHI 610 DNI 923 Diff 84	GHI 881 DNI 986 Diff 95	GHI 1050 DNI 985 Diff 88	GHI 914 DNI 973 Diff 100
Modeled values(w.m^{-2})	GHI 599 DNI 922.3 Diff 90.1	GHI 848 DNI 991 Diff 101	GHI 1054.5 DNI 981.6 Diff 103.9	GHI 918.3 DNI 978.4 Diff 101.1

B. Solar Irradiance on Slope Surfaces

The orientation and inclination of a receiver: the more sensitive to direct solar radiation values are essential information for both renewable systems and energy efficient building designs[19].

To know the optimum inclination for a maximum collection of direct solar radiation, we varied the inclination for a south oriented surface ($\gamma=0$) for specific days: Winter Solstice (22 December 2018), Autumn Equinox(23 September 2018), Summer Solstice (22 June 2018) and Spring Equinox (21 Mars 2018) as shown respectively in Figures 9,10,11,12.

The variation of the horizontal direct irradiation from the curves above “Fig.9,10,11,12”, all over the year is also much less for the inclined surface: the increase in the inclination angle of a south oriented surface lead to the reception of more irradiation during the winter than during the summer.

We can say that the optimum inclination angle range is between:

- $[40^\circ - 60^\circ]$ during winter
- $[10^\circ - 30^\circ]$ during summer
- $[30^\circ - 40^\circ]$ during spring and autumn

Which confirms the empirical rule applied to solar receiver: for maximum solar energy collection the inclination angle should be respectively 10 to 15° greater than the latitude of the site ($32^\circ 55' 46.81''\text{N}$) in Winter (for low azimuth $\gamma < 130^\circ$), 10 to 15° less than the latitude of the site in summer and approximately equal to the latitude of the site during spring and autumn as found by [20] consequently the different locations have different optimum inclination angles.

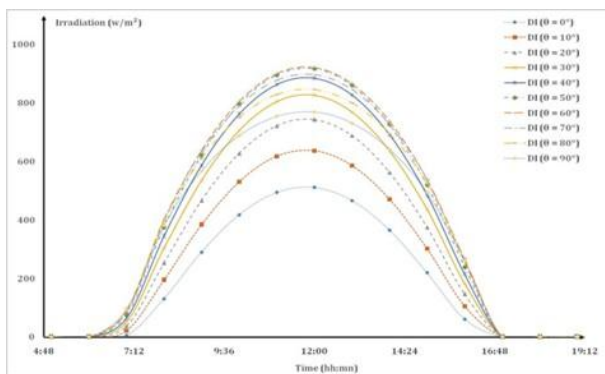


Figure 9: Estimated hourly direct radiations values for the Winter Solstice (22 December 2018): variable inclined surface oriented to the south ($\gamma=0$).

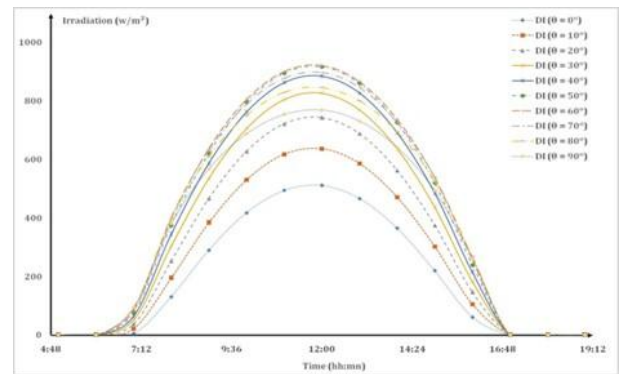


Figure 10: Estimated hourly direct radiations values for the Autumn Equinox (23 September 2018): variable inclined surface oriented to the south ($\gamma=0$).

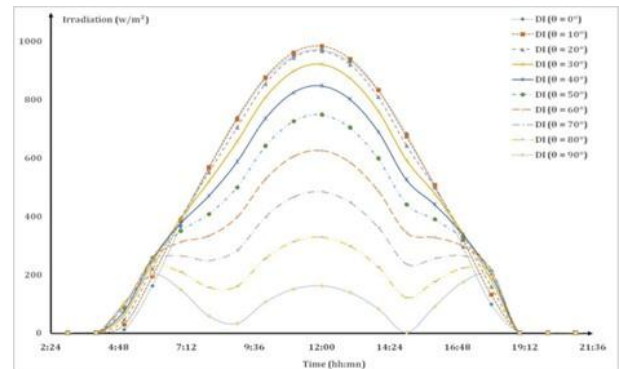


Figure 11: Estimated hourly direct irradiances values for the Summer Solstice (22 June 2018): variable inclined surface oriented to the south ($\gamma=0$).

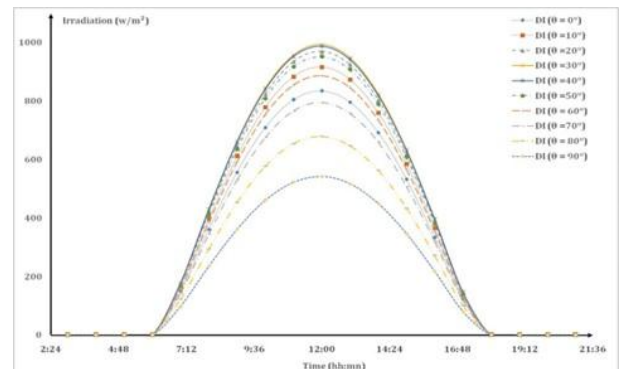


Figure 12: Estimated hourly direct irradiances values for the Spring Equinox (21 Mars 2018) variable inclined surface oriented to the south ($\gamma=0$).

Concerning the other factor that affects the incident solar radiation: the orientation of the receiver, we have set the optimum inclination angle which corresponds respectively to the shortest and the longest day of the year and we varied then the orientation angle as illustrated in Figure 13 and Figure 14

During winter, the combination of the low height of the sun with the short duration of the day gives the advantage to surface orientated between $[45^\circ, 60^\circ]$ to receive more solar irradiation compared to the other orientations. During summer the optimum orientation is the south ($\gamma=0$).

It is evident then for an optimal functioning, it is necessary to determine the optimum inclination angle and orientation of each receiver.

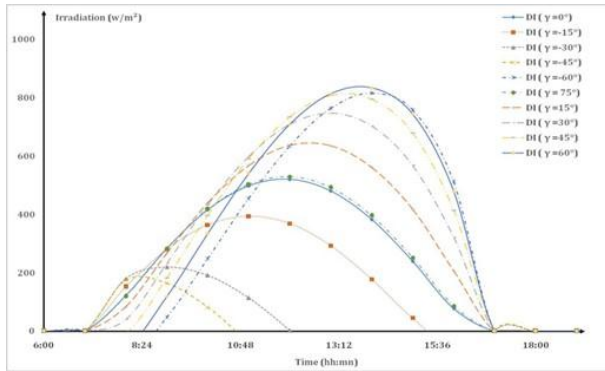


Figure 13: Minimal approach: Estimated hourly direct radiations values for the Perihelion day (2 January 2018) (inclination angle: 50°, variable orientation).

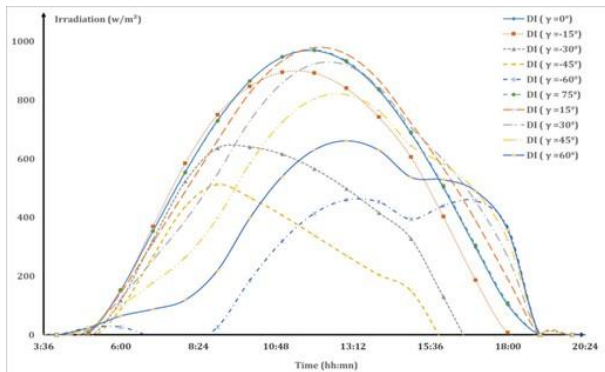


Figure 14: Maximal approach: Estimated hourly direct irradiancies values for the Aphelion day (2 July 2018) (inclination angle: 20°, orientation variable).

VI. EVALUATION METHOD AND VALIDATION

Similar studies have been carried out for different cities around the world. These studies are based on data from local metro stations and different modeling methods were used to predict solar radiation over a large area. [21], estimated the intensity of solar radiation on a tilted surface using support vector machine (SVM) and artificial neural networks (ANN). [22], used many empirical models to predict global scales of solar radiation in selected cities in China. [23], used regression and multiple regression models for the determination of horizontal solar radiation in selected cities in Turkey. [24], used clear sky and transposition models for radiation on vertical planes for Bozano Italy. Compared to these studies, ongoing work has extended the estimation to more components of solar radiation for inclined and oriented surfaces. In addition, the values are given hourly for the whole year. Table.4 can summarize our study with other similar study.

Table 3. Comparison with other similar study

Reference	[21]	[22]	[23]	[24]	Current study
City	2 sites in Saudi Arabia	Some cities in China	Some cities in Turkey	Bozano Italy	Tataouine south of Tunisia
Method	Using a support vector machine (SVM) and artificial neural networks (ANN)	Using numerous empirical models	Using regression and multi-regression models	Using a clear sky and transposition models	Using MATLAB model based on meteo station data
Kind of predicted solar radiation	solar radiation intensity on a tilted surface	solar radiation global scales	horizontal solar radiation	solar radiation on vertical planes	hourly global, direct and diffuses solar irradiation on oriented and inclined surface.

In this study we calculated the relative difference between the measured horizontal global, direct, and horizontal diffuse solar radiation and those estimated by the proposed model in clear sky conditions to evaluate the proposed model. Positive error measures indicate that the model underestimates actual radiation, while negative values indicate overestimation. The relative difference is calculated by the following formula:

$$\text{Relative difference} = 100 \times \frac{X_{\text{measured}}^i - X_{\text{calculated}}^i}{X_{\text{measured}}^i} \quad \text{Eq.16}$$

Where X_{measured}^i and $X_{\text{calculated}}^i$ are the measured and calculated values.

We established statistical error parameters to evaluate the proposed model's performance. We have used the mean absolute bias error (MBE), mean absolute percentage error (MAPE), root mean square error (RMSE), relative root mean square error (RRMSE), test statistical (TS), and coefficient of determination (R^2).

The equations of these performance indicators are provided below:

$$\text{MBE} = \sum_{i=1}^N \frac{X_{\text{measured}}^i - X_{\text{calculated}}^i}{N} \quad \text{Eq.17}$$

$$\text{MAPE} = \frac{100}{N} \times \sum_{i=1}^N \left| \frac{X_{\text{measured}}^i - X_{\text{calculated}}^i}{X_{\text{measured}}^i} \right| \quad \text{Eq.18}$$

$$\text{RMSE} = \sqrt{\frac{1}{N} \times \sum_{i=1}^N (X_{\text{measured}}^i - X_{\text{calculated}}^i)^2} \quad \text{Eq.19}$$

$$\text{RRMSE} = 100 \times \frac{\sqrt{\frac{1}{N} \times \sum_{i=1}^N (X_{\text{measured}}^i - X_{\text{calculated}}^i)^2}}{\bar{X}_{\text{measured}}^i} \quad \text{Eq.20}$$

$$R^2 = 1 - \frac{\sum_{i=1}^N (X_{\text{measured}}^i - X_{\text{calculated}}^i)^2}{\sum_{i=1}^N (\bar{X}_{\text{measured}}^i - X_{\text{measured}}^i)^2} \quad \text{Eq.21}$$

$$S = \sqrt{\frac{(N-1) \times (\text{MBE})^2}{(\text{RMSE})^2 - (\text{MBE})^2}} \quad \text{Eq.22}$$

Where N is the total number of measured data, X_{measured}^i , $X_{\text{calculated}}^i$ and $\bar{X}_{\text{measured}}^i$ are respectively the i^{th} measured value, i^{th} calculated value and the mean of measured value.

VII. PERFORMANCES OF THE CALCULATION

The relative difference between the measured data and those estimated by the proposed model when the sky is clear for studied position are shown in the Fig. 15, 16 and 17. According to the curves, the diffuses, horizontal global and direct normal irradiation are super estimated by an acceptable value not exceeded to 10% in the major of the data except for the relative lower irradiation and underestimated by at least 5% for the relative higher value of irradiation.

Table 4. Statistics performance of the proposed model.

	MBE	MAPE	RMSE	RRMSE	TS	R ²
GHI	15,9749255	4,57745438	24,6612468	4,18374084	27,2356771	0,98896212
DNI	28,1176094	6,38975983	36,5876568	5,4159267	38,4715195	0,96933038
Diff	9,66029656	5,78276568	12,6594429	7,6927844	37,8199327	0,97356294

The MBE, RMSE, RRMSE, MAPE, TS and R² values of global horizontal (GHI), direct normal (DNI) and horizontal diffuses (Diff) irradiation are illustrated in Table 3. MBE, the performance evaluation factor, yielded a slightly lower value. Certain error parameters have slightly higher values for cloudy skies than for clear skies.

Except in the case of cloudy skies, the RMSE and MAPE obtained values for clear skies are uniform and less than 15%. We can say that the obtained values of performance evaluation factor: MBE, MAPE, RMSE and TS are acceptable which indicates that the calculation in this study have worked has generalized well for clear skies.

In addition, according to the acceptable value of the determination value (R²) (up to 0.9) and the RRMSE (inferior to 5% for global and direct irradiation and about 7% for diffuses irradiation), it can be seen that the calculated horizontal global, direct normal, and diffuses irradiation for clear skies during all seasons of the year are nearly superimposed with that measured by the high precision meteorological station.

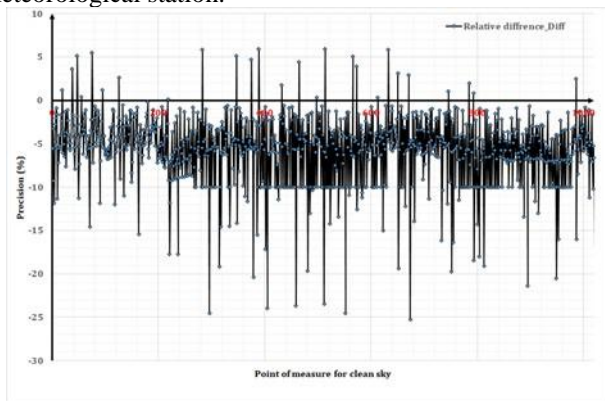


Figure 15. The relative difference between the measured and the estimated data of the horizontal diffuses irradiation (Diff) for clear sky during 2018.

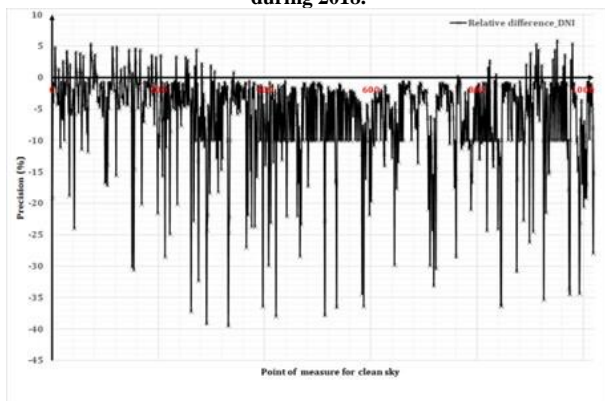


Figure 16. The relative difference between the measured and the estimated data of the direct normal irradiation (DNI) for clear sky during 2018.

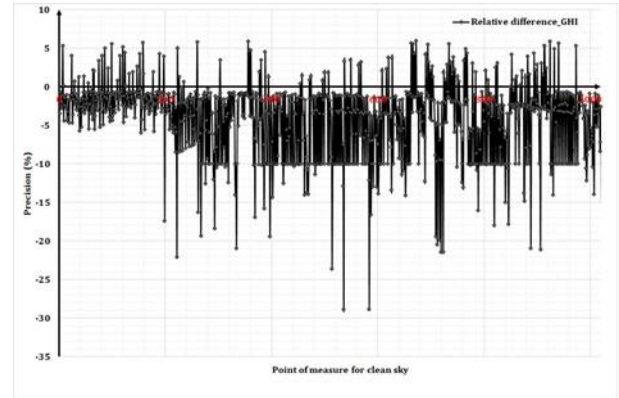


Figure 17. The relative difference between the measured and the estimated data of the horizontal global irradiation (GHI) for clear sky during 2018.

As a result, the use of this model provides a good estimate of solar radiation in Tataouine, Tunisia's south.

VIII. CONCLUSIONS

In this paper, we proposed a model that simulates global, direct, and diffuse solar radiations under clear sky conditions. The results were compared to the meteorological data given by the High Precision Meteorological Station of Tataouine. It shows a good agreement between recorded and simulated data. In addition, the influence of the various inclined surfaces facing different orientations showed that the solar radiation intensity on surfaces has presented a large variety: The optimum inclination angle was found equal to latitude + 15° for winter season, latitude - 15° for summer season and nearly equal to the latitude during the rest of the year.

The Orientation between [45°, 60°] in the winter and south facing receiver in summer collects the maximum of the incident solar radiation.

The obtained results having acceptable values of performance factor could serve as references for the solar application. It could be recommended to predict global solar radiation at Tataouine and at other different localizations. This method which is easily functional enables the clear sky estimation and model comparison at user's choice. Such accurate knowledge is also useful for the site selection of solar power plants for both photovoltaic and concentrated thermal systems.

As perspectives of this study, we propose to make modeling and experimental studies to determine the daily hourly variations from morning to evening of the scattered solar radiation spectral densities according to the wavelengths. These data are very useful and much sought after in recent research for the development of new generation photovoltaic cells with good performance that use

the splitting system or in the applications of Photovoltaic Thermal Hybrid concentrators.

ACKNOWLEDGEMENTS

The authors are grateful to the EnerMina project and the high-precision meteorological station of Tataouine for providing the solar radiation data.

REFERENCES

- [1] J. Hofierka and M. Sári, "The solar radiation model for Open source GIS: implementation and applications," *Open source GIS - GRASS users Conf.*, no. September, 2002.
- [2] J. Zhang, L. Zhao, S. Deng, W. Xu, and Y. Zhang, "A critical review of the models used to estimate solar radiation," *Renewable and Sustainable Energy Reviews*, vol. 70, 2017.
- [3] S. C. Nwokolo and J. C. Ogbulezie, "A qualitative review of empirical models for estimating diffuse solar radiation from experimental data in Africa," *Renewable and Sustainable Energy Reviews*, vol. 92, 2018.
- [4] R. G. Makade, S. Chakrabarti, B. Jamil, and C. N. Sakhale, "Estimation of global solar radiation for the tropical wet climatic region of India: A theory of experimentation approach," *Renew. Energy*, vol. 146, 2020.
- [5] M. Blal *et al.*, "A prediction models for estimating global solar radiation and evaluation meteorological effect on solar radiation potential under several weather conditions at the surface of Adrar environment," *Meas. J. Int. Meas. Confed.*, vol. 152, 2020.
- [6] Kurniawan A. Shintaku E., "Estimation of the Monthly Global, Direct, and Diffuse Solar Radiation in Japan Using Artificial Neural Network," *Int. J. Mach. Learn. Comput.*, 2020.
- [7] M. Balghouthi, S. E. Trabelsi, M. Ben Amara, A. B. H. Ali, and A. Guizani, "Potential of concentrating solar power (CSP) technology in Tunisia and the possibility of interconnection with Europe," *Renewable and Sustainable Energy Reviews*, vol. 56, 2016.
- [8] F. Kasten, "The linke turbidity factor based on improved values of the integral Rayleigh optical thickness," *Sol. Energy*, vol. 56, no. 3, 1996.
- [9] F. Kasten and A. T. Young, "Revised optical air mass tables and approximation formula," *Appl. Opt.*, vol. 28, no. 22, 1989.
- [10] L. T. Wong and W. K. Chow, "Solar radiation model," *Appl. Energy*, vol. 69, no. 3, 2001.
- [11] Y. El Mghouchi, A. El Bouardi, Z. Choulli, and T. Ajzoul, "New model to estimate and evaluate the solar radiation," *Int. J. Sustain. Built Environ.*, vol. 3, no. 2, 2014.
- [12] G. S. Campbell and J. M. Norman, "Radiation Fluxes in Natural Environments," in *An Introduction to Environmental Biophysics*, 1998.
- [13] J. A. Duffie and W. A. Beckman, *Solar Engineering of Thermal Processes: Fourth Edition*. 2013.
- [14] J. A. Bedel, J. Jan, and S. Janicot, "Diffuse Sky Radiation on Tilted Surfaces," in *Solar Radiation Data*, 1983.
- [15] Y. El Mghouchi, E. Chham, M. S. Krikiz, T. Ajzoul, and A. El Bouardi, "On the prediction of the daily global solar radiation intensity on south-facing plane surfaces inclined at varying angles," *Energy Convers. Manag.*, vol. 120, 2016.
- [16] L. Diabaté, J. Remund, and L. Wald, "Linke turbidity factors for several sites in Africa," *Sol. Energy*, vol. 75, no. 2, 2003.
- [17] C. Gueymard, "Critical analysis and performance assessment of clear sky solar irradiance models using theoretical and measured data," *Sol. Energy*, vol. 51, no. 2, 1993.
- [18] P. Ineichen and R. Perez, "A new airmass independent formulation for the linke turbidity coefficient," *Sol. Energy*, vol. 73, no. 3, 2002.
- [19] P. Talebizadeh, M. A. Mehrabian, and M. Abdolzadeh, "Prediction of the optimum slope and surface azimuth angles using the Genetic Algorithm," *Energy Build.*, vol. 43, no. 11, 2011.
- [20] K. K. Gopinathan, "Solar radiation on variously oriented sloping surfaces," *Sol. Energy*, vol. 47, no. 3, 1991.
- [21] M. A. M. Ramli, S. Twaha, and Y. A. Al-Turki, "Investigating the performance of support vector machine and artificial neural networks in predicting solar radiation on a tilted surface: Saudi Arabia case study," *Energy Convers. Manag.*, vol. 105, pp. 442–452, 2015.
- [22] L. Feng, A. Lin, L. Wang, W. Qin, and W. Gong, "Evaluation of sunshine-based models for predicting diffuse solar radiation in China," *Renewable and Sustainable Energy Reviews*, vol. 94, 2018.
- [23] I. Ustun, C. Karakus, and H. Yagli, "Empirical models for estimating the daily and monthly global solar radiation for Mediterranean and Central Anatolia region of Turkey," *Int. J. Glob. Warm.*, vol. 20, no. 3, pp. 249–275, 2020.
- [24] D. Paul, G. De Michele, B. Najafi, and S. Avesani, "Benchmarking clear sky and transposition models for solar irradiance estimation on vertical planes to facilitate glazed facade design," *Energy Build.*, vol. 255, p. 111622, 2022.